Supporting Information

Lupo et al. 10.1073/pnas.1103802108

SI Materials and Methods

Zebrafish. Transgenic and mutant lines used were: *Tg(fli1a:EGFP)*^{y5} (1); *Tg(-7.2sox10:EGFP)*^{zf77} (2); and *noi*^{tu29a} (no isthmus, a null allele of *pax2a*) (3).

Treatments with AGN194310 (AGN) or RA. Both AGN and RA affected long-term survival of treated embryos because of the known effects of retinoic acid receptor (RAR) signaling on heart development (4). For AGN, optimal survival (up to 100%) until 48–50 h postfertilization (hpf) was obtained by raising embryos at 25 °C. Later survival until 60 hpf was obtained by starting treatments at the 6-somite stage (6s) and decreasing AGN doses to 2.5–5 µM. Molecular analyses were usually performed on embryos treated with 10 µM doses from 3s, unless specifically indicated. No obvious differences in phospho-histone H3 or TUNEL staining were observed between the eye region of AGN-treated and control embryos at 32 hpf and 48 hpf, indicating that the observed eye phenotype and changes in gene expression are not attributable to major changes in the rate of cell proliferation or death. The efficiency and the specificity of AGN treatments was confirmed by using a *RARE-YFP* transgenic zebrafish line, where YFP is expressed under the control of three RA responsive elements (RAREs) (5). Reporter expression at 26 hpf was eliminated by treatments with 5 µM AGN from 3s and rescued when embryos were treated with both 5 µM AGN and 0.5 µM RA, similarly to what has been previously described with other inhibitors of the RAR pathway (5).

Morpholino Antisense Oligonucleotides (MOs). FoxC1a function was abrogated by using a pair of formerly published MOs targeting the 5′ UTR and ATG (*foxC1a* MO1: 5′-GTCAAGAAGACTGAAGCAATCCACA-3′; *foxC1a* MO2: 5′-CCTGCATGACTGCTCTCCAAAACGG-3′), which affected somitogenesis as previously described (Fig. S12*C*) (6). FoxC1a is required for cell viability in periocular mesenchyme (POM) (7), raising the possibility that coloboma is an indirect consequence of cell death. However, coinjection of *foxC1a* MOs and a *p53* MO to prevent apoptosis (8) still led to coloboma (Fig. S12*D*). Nlz1 was knocked-down using a previously described MO (5′-AGAAGTCGTACCTCAATGCTCACGG-3′) directed against the E1I1 splicing junction (9). A *pitx2* MO targeting the exon 2–intron 2 splice junction of all *pitx2* isoforms (10) was designed having the sequence: 5′-TTATTTATCAAACTTACTCGGACTC-3′. Splicing inhibitory activities of *nlz1* MO and *pitx2* MO were verified by RT-PCR (Fig. S12 *A* and *B*) using primer pairs listed in Table S2. Optimal doses of *nlz1* MO caused nonspecific toxic effects, which were prevented by coinjection with a *p53* MO (5′-GCGCCATTGCTTTGCAAGAATTG-3′), as previously described (8). To confirm abrogation of Pitx2 function, *pitx2* MO-injected embryos were analyzed for pharyngeal arch and extraocular muscle development, both of which were affected similarly to *Pitx2* mutant mice (Fig. S12*C*) (11, 12).

Histology, In Situ Hybridization (ISH), and Immunocytochemistry. For histological analysis, 60- to 72-hpf embryos were fixed in 4% paraformaldehyde, embedded in Spurr resin, sectioned at 1 µm, and stained with methylene blue. ISH was performed by using published protocols (13). To make probes for ISH, I.M.A.G.E. clones for the following genes were obtained from Geneservice (http://www.geneservice.co.uk): *cyb5a* (6795485), *cyp1B1* (7920096), *dact1* (8152792), *dhrs3a* (7037372), *eya2* (7053426), *foxC1a* (6789584), *nlz1* (7405421), full-length *pitx2c* (7172060), and *rlbp1l* (4146183). *itgA5*, *nlz2*, *nr2F5*, full-length *pitx2a*, *rdh10a*, *twist1a*, and isoform-specific *pitx2a* and *pitx2c* cDNA fragments were amplified by RT-PCR from zebrafish embryo total RNA and subcloned in pGEM-T Easy (Promega) using primer pairs listed in Table S2. Partial *aldh1A2* and full-length *aldh1A3* (accession no. DQ105978) cDNAs were PCR-amplified from zebrafish embryo total RNA as previously described (14). *ptc1* was a kind gift of Phil Ingham (University of Sheffield, Sheffield, UK) (15). All other plasmids were previously described (16–18). Immunostaining of optic nerve axons was performed with an anti-acetylated tubulin antibody (Sigma) (19).

RT-PCR and Real-Time Quantitative PCR. Relative gene expression levels in different samples were determined with the relative standard curve quantification method (20) using *EF1α* (21) as a normalizer. Primers for quantitative PCR were designed using Primer3 (http://fokker.wi.mit.edu/primer3/input.htm) and are listed in Table S3. Statistical analysis of experimental data were performed with Microsoft Excel software.

1. Lawson ND, Weinstein BM (2002) In vivo imaging of embryonic vascular development using transgenic zebrafish. *Dev Biol* 248:307–318.
2. Hoffman TL, Javier AL, Campeau SA, Knight RD, Schilling TF (2007) Tfap2 transcription factors in zebrafish neural crest development and ectodermal evolution. *J Exp Zoolog B Mol Dev Evol* 308:679–691.
3. Macdonald R, et al. (1997) The Pax protein Noi is required for commissural axon pathway formation in the rostral forebrain. *Development* 124:2397–2408.
4. Lin S, et al. (2010) Endogenous retinoic acid regulates cardiac progenitor differentiation. *Proc Natl Acad Sci USA* 107:9234–9239.
5. Perz-Edwards A, Hardison NL, Linney E (2001) Retinoic acid-mediated gene expression in transgenic reporter zebrafish. *Dev Biol* 229:89–101.
6. Topczewska JM, et al. (2001) The winged helix transcription factor Foxc1a is essential for somitogenesis in zebrafish. *Genes Dev* 15:2483–2493.
7. Berry FB, et al. (2008) FOXC1 is required for cell viability and resistance to oxidative stress in the eye through the transcriptional regulation of FOXO1A. *Hum Mol Genet* 17:490–505.
8. Robu ME, et al. (2007) p53 activation by knockdown technologies. *PLoS Genet* 3:e78.
9. Hoyle J, Tang YP, Wiellette EL, Wardle FC, Sive H (2004) *nlz* gene family is required for hindbrain patterning in the zebrafish. *Dev Dyn* 229:835–846.
10. Essner JJ, Branford WW, Zhang J, Yost HJ (2000) Mesendoderm and left-right brain, heart and gut development are differentially regulated by pitx2 isoforms. *Development* 127:1081–1093.
11. Liu W, Selever J, Lu MF, Martin JF (2003) Genetic dissection of Pitx2 in craniofacial development uncovers new functions in branchial arch morphogenesis, late aspects of tooth morphogenesis and cell migration. *Development* 130:6375–6385.
12. Diehl AG, et al. (2006) Extraocular muscle morphogenesis and gene expression are regulated by Pitx2 gene dose. *Invest Ophthalmol Vis Sci* 47:1785–1793.
13. Thisse C, Thisse B (2008) High-resolution in situ hybridization to whole-mount zebrafish embryos. *Nat Protoc* 3:59–69.
14. Lupo G, et al. (2005) Dorsoventral patterning of the *Xenopus* eye: A collaboration of Retinoid, Hedgehog and FGF receptor signaling. *Development* 132:1737–1748.
15. Concordet JP, et al. (1996) Spatial regulation of a zebrafish patched homologue reflects the roles of sonic hedgehog and protein kinase A in neural tube and somite patterning. *Development* 122:2835–2846.
16. Rohr KB, Barth KA, Varga ZM, Wilson SW (2001) The nodal pathway acts upstream of hedgehog signaling to specify ventral telencephalic identity. *Neuron* 29:341–351.
17. Take-uchi M, Clarke JDW, Wilson SW (2003) Hedgehog signalling maintains the optic stalk-retinal interface through the regulation of Vax gene activity. *Development* 130:955–968.
18. McMahon C, Gestri G, Wilson SW, Link BA (2009) Lmx1b is essential for survival of periocular mesenchymal cells and influences Fgf-mediated retinal patterning in zebrafish. *Dev Biol* 332:287–298.
19. Wilson SW, Ross LS, Parrett T, Easter SS, Jr. (1990) The development of a simple scaffold of axon tracts in the brain of the embryonic zebrafish, *Brachydanio rerio*. *Development* 108:121–145.
20. Cikos S, Bukovská A, Koppel J (2007) Relative quantification of mRNA: Comparison of methods currently used for real-time PCR data analysis. *BMC Mol Biol* 8:113.
21. Vitorino M, et al. (2009) Vsx2 in the zebrafish retina: Restricted lineages through derepression. *Neural Dev* 4:14.

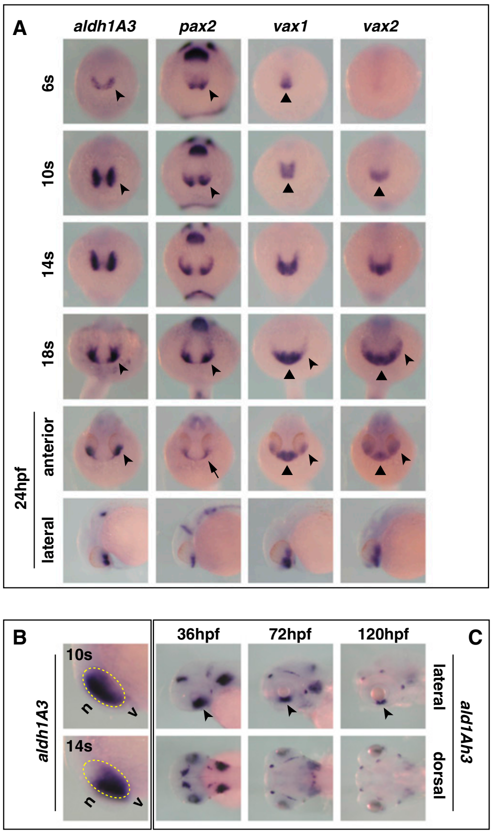

Fig. S1. Expression pattern of *aldh1A3* during zebrafish development. (*A*) Frontal/dorsal (6s–18s and 24 hpf, top row) or lateral (24 hpf, bottom row) views of wild-type embryos hybridized with the indicated probes, showing that *aldh1A3* is expressed at the right time and place to take part in ventral optic cup morphogenesis by comparison with other known regulators of ventral eye development. During early somitogenesis, expression of *aldh1A3* and *pax2* becomes detectable in the eye field (arrowheads), whereas *vax1* and *vax2* expression is limited to the forebrain (triangles). By 14s–18s, all these genes are expressed in the ventral eye (arrowheads), while *vax1* and *vax2* remain also expressed in the ventral forebrain (triangles). At 24 hpf, *aldh1A3*, *vax1*, and *vax2* are expressed in the ventral optic cup (arrowheads), while *pax2* expression is confined to the optic stalk (OS) (arrow). Similar to previous stages, *vax1* and *vax2* domains also include the ventral forebrain (triangles). (*B*) Lateral views of the head region of 10s or 14s embryos, showing that *aldh1A3* expression is initially detectable in the nasal (n) part of the eye but becomes localized to the ventral (v) eye as early as 14s. The yellow dashed circles highlight the eye region. (*C*) Lateral (top row) or dorsal (bottom row) of 36- to 120-hpf embryos, showing that *aldh1A3* expression is maintained in the ventral retina (VR)/OS throughout the stages of optic fissure closure (arrowheads).

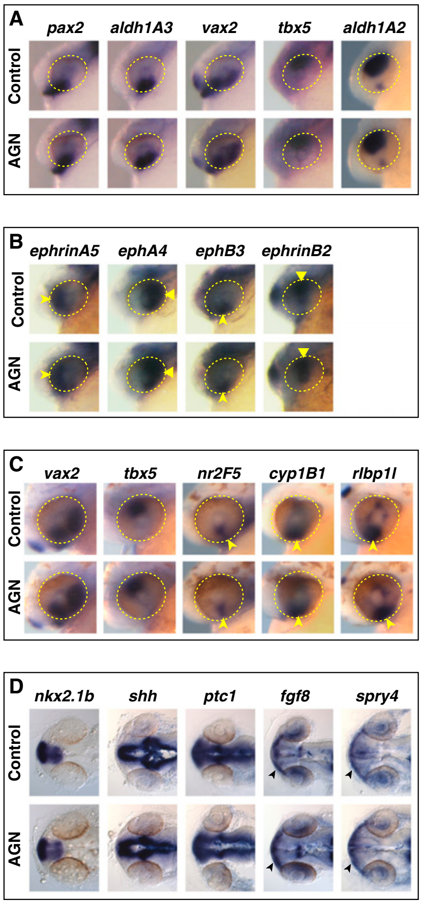

Fig. S2. RAR signaling is not required for patterning of the retina and forebrain. Embryos treated with DMSO or 10 μM AGN from 3s and hybridized at 24–25 hpf (*A*, *B*, and *D*) or 31 hpf (*C*) with the indicated probes. (*A*–*C*) Lateral views of heads. Yellow circles highlight the eye region. (*B*) Arrowheads and triangles point to the expression of *ephrinA5* and *ephA4* in the nasal or temporal retina, respectively, or to the expression of *ephB3* and *ephrinB2* in the dorsal retina and VR, respectively. (*C*) Arrowheads point to the expression of *nr2F5*, *cyp1B1*, or *rlbp1l* in the VR/OS. (*D*) Dorsal views of heads. Arrowheads point to *fgf8* or *spry4* expression in the OS.

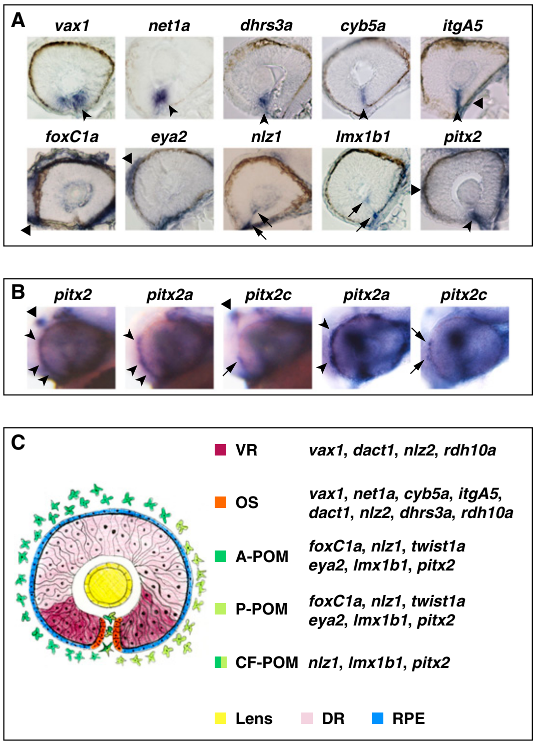

Fig. S3. Expression patterns of VR/OS and POM genes. (*A*) Histological sections of 32- to 36-hpf eyes hybridized with the indicated probes. In the upper row, arrowheads point to expression in VR/OS cells, and the triangle points to *itgA5* in extraocular tissue. In the lower row, triangles point to expression in POM around the optic cup, arrows point to expression in POM cells inside the choroid fissure, and the arrowhead points to *pitx2* expression at the level of the choroid fissure, which might include OS cells besides POM. (*B*) Lateral views of 31-hpf heads (left three images) or eyes (right two images) hybridized with a *pitx2* pan-isoform probe or with *pitx2a*- or *pitx2c*-specific probes, showing that *pitx2a* is the predominant isoform in the POM (arrowheads), whereas *pitx2c* is selectively expressed in the dorsal diencephalon (triangles). Arrows point to limited expression of *pitx2c* in few POM cells. (*C*) Schematic representation of the expression domains of VR/OS and POM genes, based on the data shown in *A*, Figs. 2 *B* and *C* and 3 *B* and *C*, and Fig. S5 *A* and *B*. A-POM, anterior POM; P-POM, posterior POM; CF-POM, POM located within the choroid fissure; DR, dorsal retina; RPE, retinal pigmented epithelium.

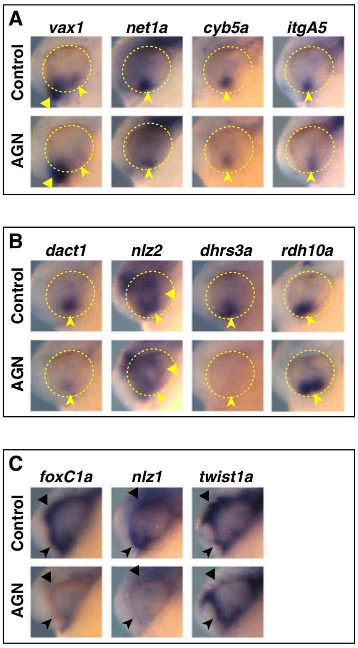

Fig. S4. RAR signaling regulates gene expression in the VR/OS and in POM. Lateral views of heads of 24- to 25-hpf embryos treated with DMSO or 10 μM AGN from 3s and hybridized with the indicated probes. (*A* and *B*) AGN treatment causes down-regulation of *vax1*, *net1a*, *cyb5a*, *itgA5*, *dact1*, *nlz2*, and *dhrs3a* and up-regulation of *rdh10a* in the VR/OS (arrowheads). Triangles point to expression of *vax1* in the ventral forebrain (*A*) and *nlz2* in the dorsal retina (*B*). (*C*) AGN treatment decreases *foxC1a* and *nlz1* expression in both anterior-ventral (arrowheads) and anterior-dorsal (triangles) POM as well as *twist1a* expression in dorsal POM only (triangles).

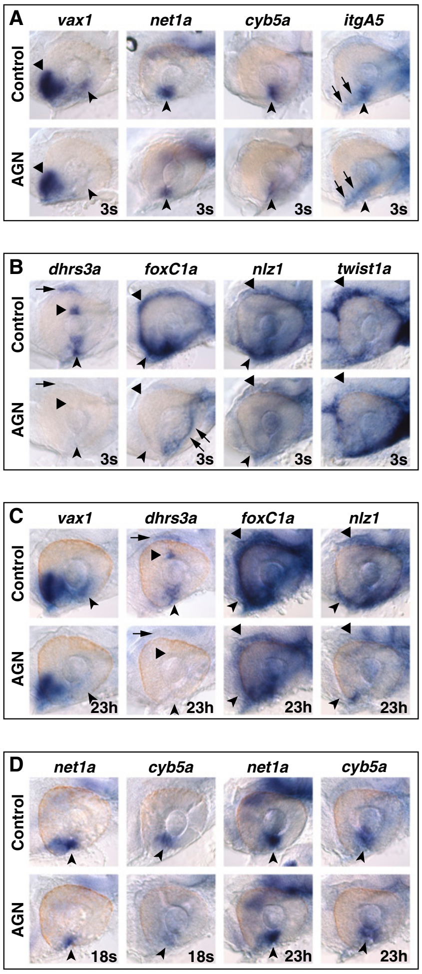

Fig. S5. RAR signaling regulates VR/OS and POM genes and is required beyond 18s to maintain their expression. Lateral views of eyes of 31-hpf hybridized embryos treated with DMSO or 10 μM AGN from 3s (*A* and *B*) or from 18s or 23 hpf (23h) (*C* and *D*), as indicated. (*A*) AGN treatment causes down-regulation of *vax1*, *net1a*, *cyb5a*, and *itgA5* in VR/OS cells (arrowheads). Triangles point to *vax1* expression in the ventral forebrain. Arrows point to *itgA5* expression in extraocular tissue at the back of the eye. (*B*) In the control eye, *dhrs3a* is expressed in VR/OS cells (arrowhead), in the dorsal retina (triangle), and in dorsal POM (arrow). All these domains are down-regulated in the AGN-treated embryo. AGN treatment decreases *foxC1a* and *nlz1* expression in both anterior-ventral (arrowheads) and anterior-dorsal (triangles) POM, although residual *foxC1a* staining is detectable in a ventro-medial location at the back of the eye (arrows). AGN treatment decreases *twist1a* expression in dorsal POM only (triangles). (*C*) Embryos treated with DMSO or AGN from 23 hpf show that AGN treatment causes down-regulation of *vax1* and *dhrs3a* in the VR/OS (arrowheads) and of *dhrs3a* in the dorsal retina (triangle) and in dorsal POM (arrow). *foxC1a* and *nlz1* expression in both anterior-ventral (arrowheads) and anterior-dorsal (triangles) POM is decreased in the AGN-treated embryos. (*D*) Embryos treated with DMSO or AGN from 18s or from 23 hpf showing decreased expression of both *net1a* and *cyb5a* in the VR/OS (arrowheads) only in the embryos treated with AGN from 18s.

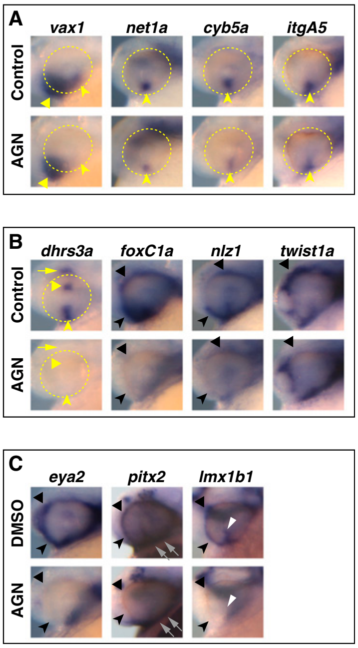

Fig. S6. RAR signaling regulates gene expression in the VR/OS and in POM. Lateral views of heads of 31-hpf embryos treated with DMSO or 10 μM AGN from 3s and hybridized with the indicated probes. (*A*) AGN treatment causes down-regulation of *vax1*, *net1a*, *cyb5a*, and *itgA5* in VR/OS cells (arrowheads). Triangles point to *vax1* expression in the ventral forebrain. (*B*) In the control eye, *dhrs3a* is expressed in VR/OS cells (arrowhead), in the dorsal retina (triangle), and in dorsal POM (arrow). All these domains are down-regulated in the AGN-treated embryo. AGN treatment decreases *foxC1a* and *nlz1* expression in both anterior-ventral (arrowheads) and anterior-dorsal (triangles) POM as well as *twist1a* expression in dorsal POM only (triangles). (*C*) AGN treatment decreases *eya2*, *pitx2*, and *lmx1b1* expression in anterior-ventral (arrowheads) and/or anterior-dorsal (black triangles) POM. Expression of *lmx1b1* within the choroid fissure is also diminished (white triangles). *pitx2* is strongly expressed in extraocular mesodermal tissue in both the controls and the AGN-treated embryo (arrows).

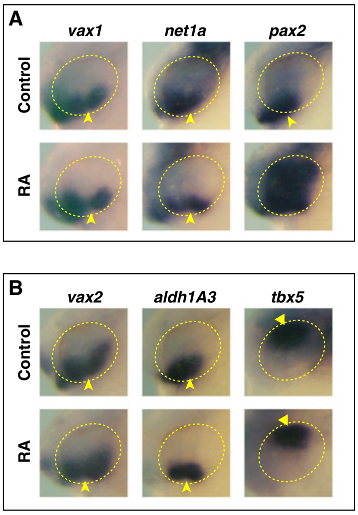

Fig. S7. Effects of exogenous RA on eye dorsoventral (DV) polarity. (*A* and *B*) Lateral views of heads of 25 to 26 hpf embryos treated with DMSO or 0.25 μM RA from 3s and hybridized with the indicated probes. RA treatment up-regulates *pax2*, but not *vax1*, *net1a*, *vax2*, or *aldh1A3* expression in the dorsal eye. Arrowheads point to expression in the VR/OS. RA treatment causes no evident effects on *tbx5* expression in the dorsal eye (triangles).

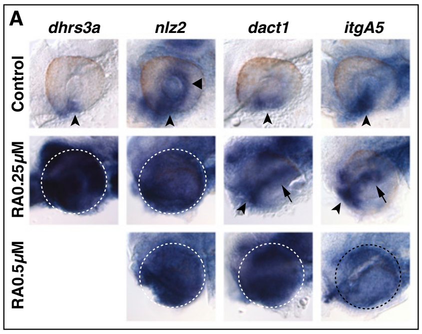

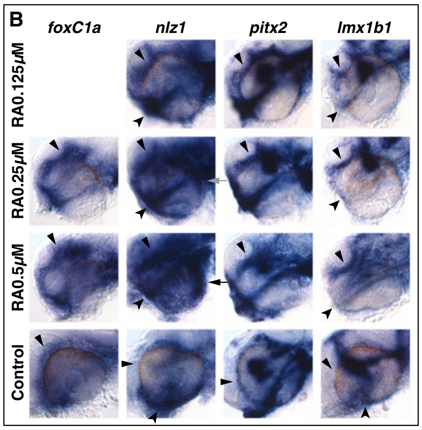

Fig. S8. Exogenous RA increases expression of VR/OS and POM genes. (*A* and *B*) Lateral views of eyes from 25- to 29-hpf hybridized embryos treated with DMSO or 0.125–0.5 μM RA from 3s. (*A*) In the control eyes, *dhrs3a*, *nlz2*, *dact1*, and *itgA5* are expressed in VR/OS cells (arrowheads). *nlz2* also has a restricted expression domain in the dorsal retina (triangle). RA treatments cause up-regulation of all these genes in the dorsal retina. Arrows point to partial *dact1* and *itgA5* up-regulation in the central retina region at lower RA doses. Dashed circles highlight the eye region in treated embryos. (*B*) RA treatments increase *foxC1a*, *nlz1*, *lmx1b1*, and *pitx2* expression in anterior POM (triangles). The RA-treated embryos also show dose-dependent decrease in *nlz1* and *lmx1b1* expression in ventral POM (arrowheads). Arrows point to up-regulation of *nlz1* in the dorsal eye region of the RA-treated embryos.

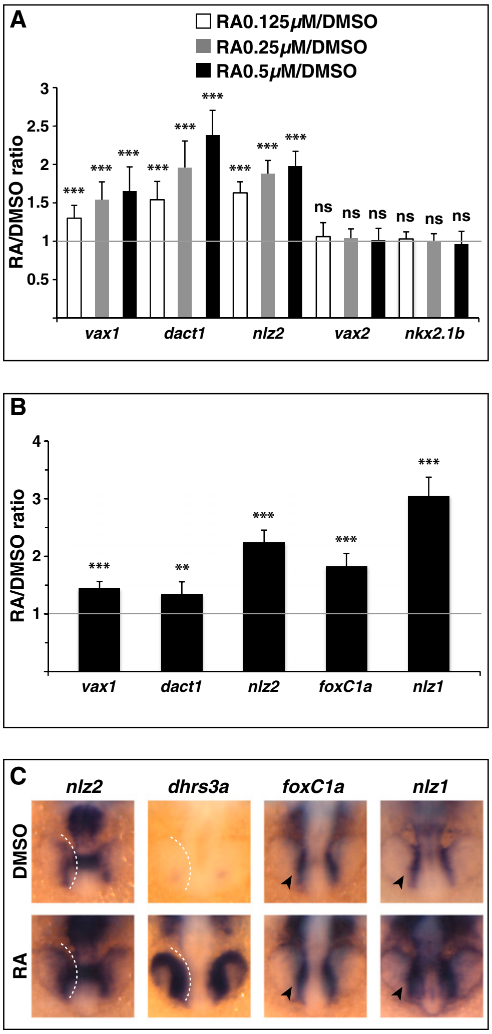

Fig. S9. Early response genes to up-regulated RA signaling. (*A*) Real-time PCR quantification of gene expression in 25- to 26-hpf whole embryos after embryo treatments with the indicated reagents from 3s, shown as the mean ratio between RA and DMSO conditions in 10 biological replicates. Error bars show SDs. $***P < 0.001$; ns, nonsignificant ($P \geq 0.05$) according to two-tailed Student's *t* test. (*B* and *C*) Embryos at 18s were incubated in DMSO or 0.5 μM RA for 30–50 min and harvested for gene expression analysis by real-time PCR (*B*) or ISH (*C*). (*B*) Results of real-time PCR quantification shown as the ratio between RA and DMSO conditions and representing the mean of eight biological replicates for *vax1*, *dact1*, and *foxC1a* or six biological replicates for *nlz2* and *nlz1*. Error bars show SDs. $**P < 0.01$; $***P < 0.001$ according to two-tailed Student's *t* test. (*C*) Dorsal/anterior views of heads of 18s whole embryos hybridized with the indicated probes. RA treatment enhances expression of *nlz2* and *dhrs3a* in the optic vesicle and of *foxC1a* and *nlz1* in migrating POM cells (arrowheads). White dashed lines highlight the proximal edge of the optic vesicle.

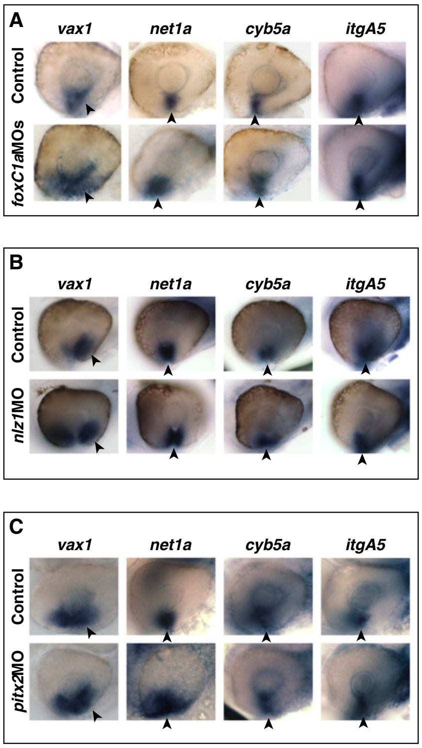

Fig. S10. Abrogation of FoxC1a, Nlz1, or Pitx2 function does not affect VR/OS gene expression. Lateral views of eyes from 31- to 32-hpf hybridized embryos showing no obvious changes in the expression of *vax1*, *net1a*, *cyb5a*, and *itgA5* in the VR/OS (arrowheads) between the controls and the embryos injected with *foxC1a* MO (*A*), *nlz1* MO (*B*), or *pitx2* MO (*C*).

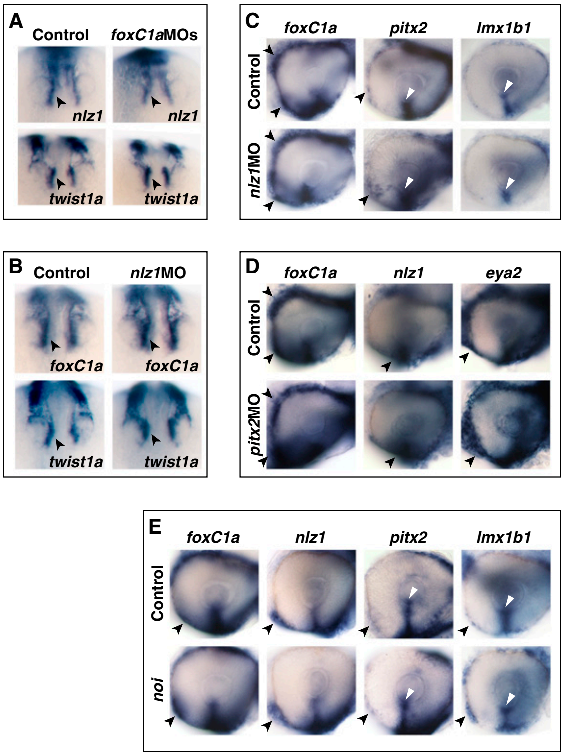

Fig. S11. Expression patterns of POM genes in POM gene morphants. (*A*) Frontal/dorsal views of 20s hybridized embryos showing no differences in the expression of *nlz1* and *twist1a* in migrating POM (arrowheads) between the controls and the *foxC1a* MO-injected embryos. (*B*) Frontal/dorsal views of 22s hybridized embryos showing no differences in the expression of *foxC1a* and *twist1a* in migrating POM (arrowheads) between the controls and the *nlz1* MO-injected embryos. (*C* and *D*) Lateral views of eyes from 31- to 32-hpf hybridized controls or embryos injected with the indicated MOs. (*C*) *foxC1a*, *pitx2*, and *lmx1b1* expression in anterior POM (arrowheads) and/or within the choroid fissure (white triangles) is not affected in the *nlz1* MO-injected embryos. (*D*) Expression of *foxC1a*, *nlz1*, and *eya2* in anterior POM (arrowheads) is not affected in the *pitx2* MO-injected embryos. (*E*) Lateral views of eyes from 32-hpf hybridized controls or *noi* embryos showing no appreciable differences in the expression of *foxC1a*, *nlz1*, *pitx2*, and *lmx1b1* in anterior POM (arrowheads) and/or within the choroid fissure (white triangles).

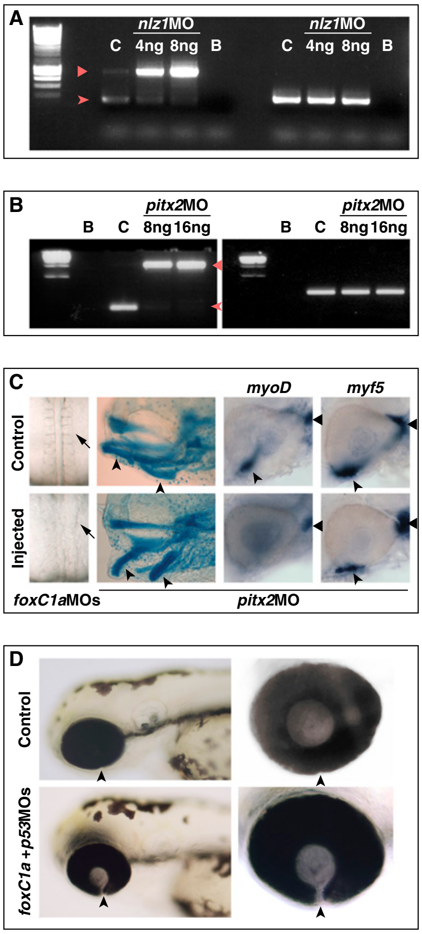

Fig. S12. Controls for the activity of MOs against POM genes. (*A*) RT-PCR on RNA from 30-hpf controls (C) or embryos injected with 4 ng (M4) or 8 ng (M8) of *nlz1* MO, showing disrupted splicing of *nlz1* mRNA (left lanes). Wild-type RNA is nearly absent in *nlz1* morphants and replaced by immature mRNA retaining the first intron, which is predicted to contain an in-frame stop codon after 39 bp. The arrowhead and triangle point to the spliced and nonspliced *nlz1* PCR products, respectively. *EF1*α (right lanes) was used as a loading control. B, blank reactions. (*B*) RT-PCR on RNA from 30-hpf controls (C) or embryos injected with 8 ng (M8) or 16 ng (M16) of *pitx2* MO, showing disrupted splicing of *pitx2* mRNA (left lanes). Wild-type RNA was nearly absent in *pitx2* morphants and replaced by immature mRNA retaining the second intron, which is predicted to contain an in-frame stop codon after 30 bp, leading to a truncated protein lacking the last 14 aa in the homeodomain and the whole C-terminal region. The arrowhead and triangle point to the spliced and nonspliced *pitx2* PCR products, respectively. *EF1*α (right lanes) was used as a loading control. B, blank reactions. (*C Left*) Disrupted somitogenesis in a 18s embryos injected with *foxC1a* MOs. (*Center*) Abnormal visceral arch morphogenesis in a 4-d-old embryo injected with *pitx2* MO, as shown by cartilage staining (arrowheads point to derivatives of the first two arches). (*Right*) Eyes of 32-hpf hybridized controls or *pitx2* MO-injected embryos showing reduction of *myoD*-positive ventral extraocular muscles (arrowheads), but not dorsal *myoD*-positive muscles (triangles) or *myf5*-positive muscles, in the *pitx2* morphants. (*D*) Coloboma in *foxC1A* morphants is not caused by apoptosis. Lateral views (*Left*) of the head region of 72-hpf control embryos or embryos that were injected with a combination of *foxC1a* MOs and *p53* MO. The choroid fissure (arrowheads) is not closed in embryos coinjected with *foxC1a* MOs and *p53* MO. (*Right*) Images are higher magnifications of the eyes.

Table S1. List of genes downstream of RAR signaling during zebrafish eye morphogenesis and the effects on their expression of the different functional manipulations used in this study

Name	Role	Domain	AGN	RA	*foxC1a* MOs	*nlz1* MO	*pitx2* MO	*noi*	Coloboma
vax1	TF	VR/OS	↓	↑	NC	NC	NC	NC	Yes
nlz2	TF	VR/OS	↓	↑	ND	ND	ND	NC	Yes
dact1	Intracell.	VR/OS	↓	↑	ND	ND	ND	NC	ND
net1a	Secreted	VR/OS	↓	NC	NC	NC	NC	↓	ND
itga5	TM	VR/OS	↓	↑	NC	NC	NC	↓	ND
cyb5a	Metab.	VR/OS	↓	ND	NC	NC	NC	↓	ND
dhrs3a	Metab.	VR/OS	↓	↑	ND	ND	ND	NC	ND
rdh10a	Metab.	VR/OS	↑	ND	ND	ND	ND	NC	ND
foxc1a	TF	POM	↓	↑	ND	NC	NC	NC	Yes
nlz1	TF	POM	↓	↑	NC	ND	NC	NC	Yes
twist1a	TF	POM	↓	ND	NC	NC	ND	ND	ND
eya2	TF	POM	↓	↑	↓	↓	NC	ND	ND
pitx2	TF	POM	↓	↑	↓	NC	ND	NC	Yes
lmx1b1	TF	POM	↓	↑	↓	NC	↓	NC	Yes

Up (↑) or down (↓) arrows indicate up-regulation or down-regulation effects, respectively. The effects of RA treatments on *vax1* and *net1a* varied with increasing doses of RA. The "Coloboma" column indicates whether gene function abrogation by MOs in zebrafish embryos causes coloboma. See text for details. Intracell., intracellular molecule; Metab., metabolic enzyme; NC, not changed; ND, not determined; TF, transcription factor; TM, transmembrane molecule.

Table S2. List of primers used in this study for RT-PCRs

Name	Forward primer (5′ → 3′)	Reverse primer (5′ → 3′)
nlz1	ACAAGTCACATACTTCACCC	CAGGTCTGAGCCAGCAATGC
pitx2a	CCACTCTCTGCGTCTTTGC	AGCACACGTTGATGCAAGTT
pitx2c	TGTGCAGGAGAGTGTGTGTG	GGAGGTGTCTGAAACCGTGT
pitx2a full-length	CCACTCTCTGCGTCTTTGC	CAATGGAGCCTTTGCCTTC
pitx2 exon 2–exon 3	CTGGAGGCCACTTTTCAGAG	CGTCGATTCTTGAACCACAC
itgA5	CAGAGTCTGCAGCGATACCA	TTCCTCCGCCGTCTACTCTA
nlz2	ATTGGGTCATGATCACATCG	CACGGATCCAGTCCTTCAGT
nr2F5	GAGGATTTCCCACGCAATAA	GCCTCTGCAGGAAACAGTTC
rdh10	CACGGCATTAAACATGGTGAT	CAAATGCAAGTGCACCAGTC
twist1a	GACTCAGGGAAGCCACGAC	CACCAGATCTATTCTGCATTGTG

Table S3. List of primers used in this study for real-time PCRs

Name	Forward primer (5′ → 3′)	Reverse primer (5′ → 3′)
cyb5a	ATTGCCAAACCACCAGAATC	TGCCTCCTCTGCAGTGTAAA
dact1	TAGGGTGCGACCAATGAAAT	ATTTGACTTCCCAGCTGACC
dhrs3a	CAGGAGCTGCTTGACTGTTG	CTTGGGACAACAAGCCATCT
foxC1a	TTTACTACCCCGTGGTGGAC	CGTCTGACGCATTTCAACAC
lmx1b1	GGACGTCCAGAAGCTGACAT	TTCTCCCTCTCCACAAGTCC
nlz1	CCACAGCGCCCTACTATTCT	ATCCTGCTTGTTCCTGTGCT
nlz2	ATCAGCGCTTGGATACCAGT	CACGGATCCAGTCCTTCAGT
nkx2.1b	GTACGACAGGTGGATGCAGA	TCACTTCTCCCTCCGAGAAA
rdh10a	ACAACAACGAGGCCAAGAAC	TTCTGCCCTCTCAGTGGTCT
pitx2a	ACTTGCATCAACGTGTGCTC	AAAAGTGGCCTCCAGTTCCT
pitx2c	CCTCCAGTCCAGAGTCCGTA	AAAAGTGGCCTCCAGTTCCT
vax1	TCTGCAGCAAACCCCTCTAC	TCGTACCCTGTTCGTCCTTC
vax2	TGGTAAGGAGGAACGTTTGG	GGCTTTCTTCACCAAACACG